Komarova et al., http://www.jcb.org/cgi/content/full/jcb.200807179/DC1

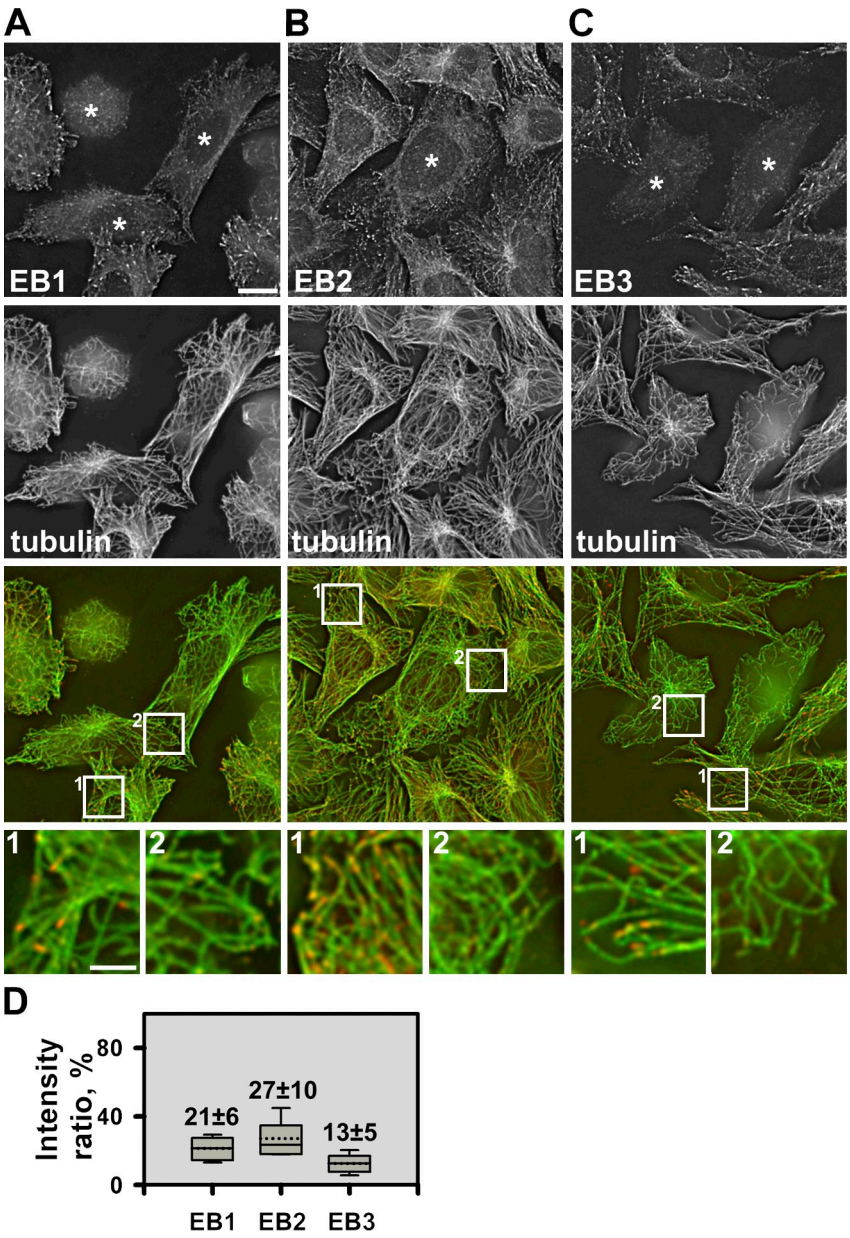

Figure S1. **Expression of EB1-CΔAc reduces the accumulation of endogenous EBs at the MT tips.** (A–C) CHO-K1 cells expressing HA-EB1-CΔAc mutant were stained for the HA tag to detect expressing cells (indicated by asterisks) for endogenous EB1 (A), EB2 (B), and EB3 (C) (red) and tubulin (green). Cells expressing HA-EB1-CΔAc mutant showed reduced levels of EBs at the MT tips. Bar, 10 μm. Enlarged parts of the non-transfected cells (box 1) and cells expressing HA-EB1-CΔAc mutant (box 2) are shown in the panels beneath. Bar, 5 μm. (D) Quantification of the accumulation of EBs at the outmost MT tips in the cells expressing HA-EB1-CΔAc mutant. Integrated intensity of EB1, EB2, and EB3 was expressed as a percentage of the intensity in control cells from the same image, which was taken for 100%. The boundaries of the box and whiskers indicate the 25th and the 75th percentile, and the 90th and 10th percentiles, respectively. The median and the mean are shown by a straight and a dotted line, respectively. Numbers on the graphs indicate the average percentage ± SD of the signal remaining at the MT tips.

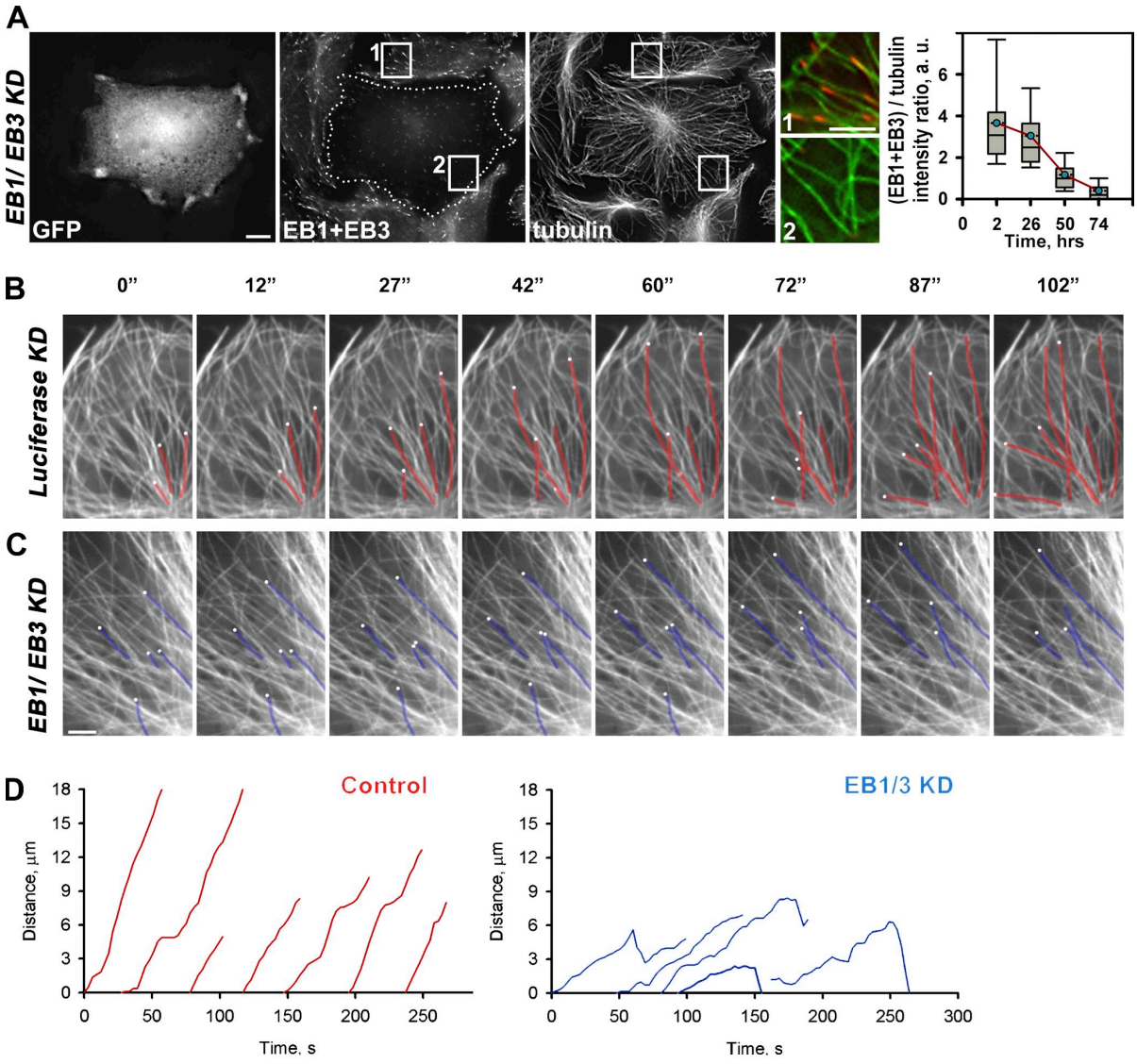

Figure S2. **Characterization of EB1/EB3-depleted cells.** (A) Simultaneous depletion of EB1 and EB3 by nuclear microinjection. A representative image of CHO-K1 cells stained for GFP, EB1 + EB3 (mixture of antibodies), and tubulin 74 h after microinjection of CFP-expressing EB1/EB3 shRNA vector. The depleted cell is indicated by a dotted line. Enlarged parts of the control and knockdown cells are shown in color; EB1 + EB3 = red; tubulin = green. Bar, 10 µm. Box graph demonstrating the intensity ratios of EB1 + EB3 to tubulin at the MT tips 2, 26, 50, and 74 h after microinjection of the shRNA construct is shown on the right. The boundaries of the box and whiskers indicate the 25th and the 75th percentile, and the 90th and 10th percentiles, respectively. The median and the mean are shown by straight lines and blue circles, respectively. The levels of the remaining EB1 + EB3 proteins expressed as a percentage of the intensity in control cells (taken as 100%) was 100 ± 11% at 2 h (114 MT tips in 13 cells), 82.42 ± 11% at 26 h (141 MT tips in 10 cells), 41± 17% at 50 h (284 MT tips in 14 cells), and at 8.8 ± 2.8% 74 h (221 MT tips in 9 cells). In all cases 95% confidence intervals are non-overlapping. (B–D) MT dynamics in CHO-K1 cells after simultaneous depletion of EB1 and EB3. (B and C) CHO-K1 cells co-expressing CFP and luciferase (A) or EB1/EB3 shRNAs (B) were microinjected with Cy3-labeled tubulin and imaged with a 3-s time interval. Several growing MTs are outlined in red (control) or blue (EB1/EB3 depletion); the position of MT plus-ends is indicated by white dots. Bar, 5 µm. (D) Representative MT life history plots (displacement of the plus-end over time) from the cells shown in B and C. (E) Visualization of MT outgrowth from the centrosome using photobleaching. Time-lapse images of a CHO-K1 cell expressing mCherry–α-tubulin before and after photobleaching (photobleached area is outlined by blue line). Several MTs growing from the centrosome are highlighted in red. Time after photobleaching is in the top left corner. Bar 5 µm.

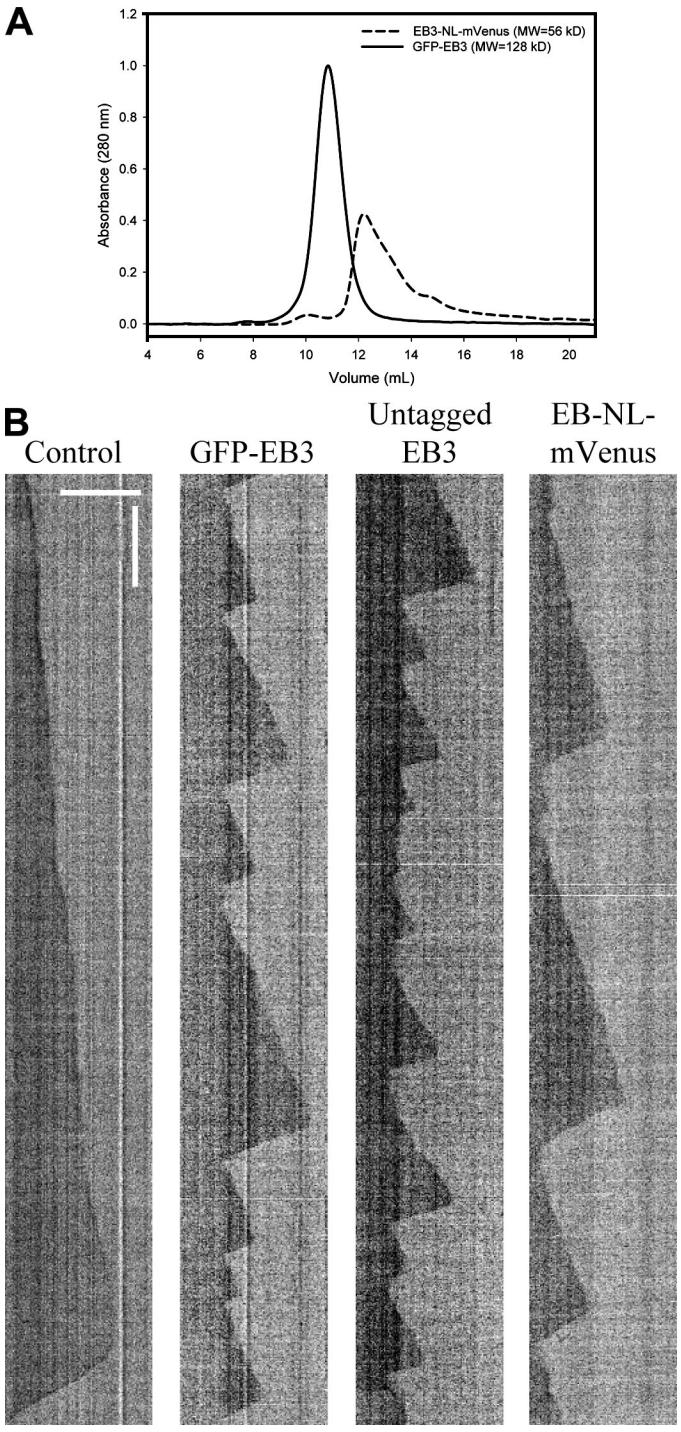

Figure S3. **Analysis of purified EB3 proteins by size-exclusion chromatography and MT dynamics in vitro.** (A) Size exclusion chromatograms of the monomeric and dimeric versions of EB3. Protein elution was monitored by absorbance at 280 nm. The protein mass of the eluted peaks was estimated by static light scattering and is indicated in the plot legend. (B) Representative kymographs of MT plus-end behavior in vitro. Different EB3 mutants (as indicated) were added to 15 μM of tubulin (control) at the concentration of 1 μM. Horizontal bar, 5 μm; vertical bar, 1 min.

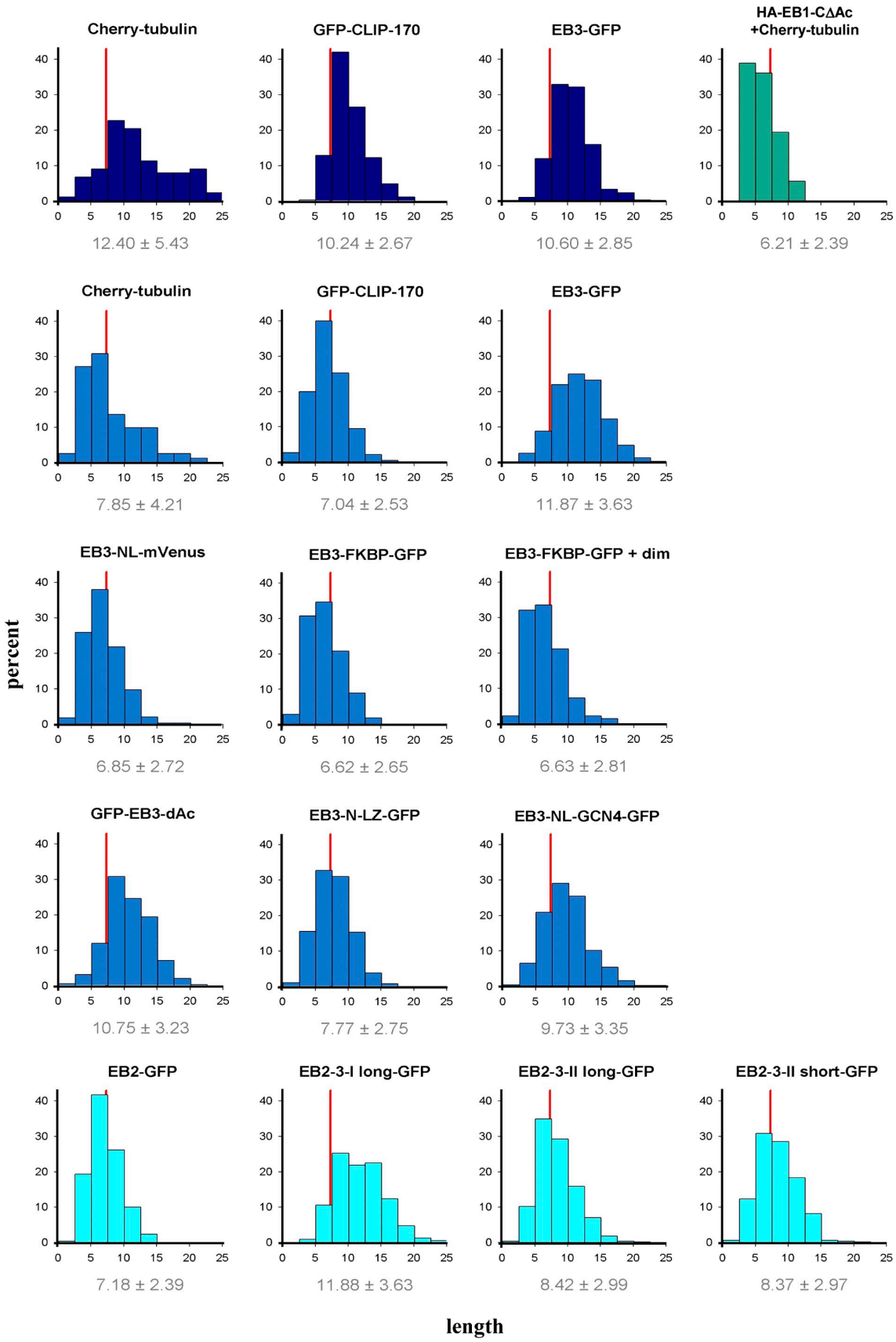

Figure S4. **Histograms of distribution of MT growth lengths in control cells, EB1/EB3-depleted cells, and after rescue with different EB3 and EB2 mutants.** The distributions of MT growth lengths that were used for calculation of the percentage of MT growth episodes longer than for 7.5 μm (red lines) presented in Fig. 7. The color code is the same as for Fig. 7. The average growth length (±SD) for each condition is indicated below the histogram.

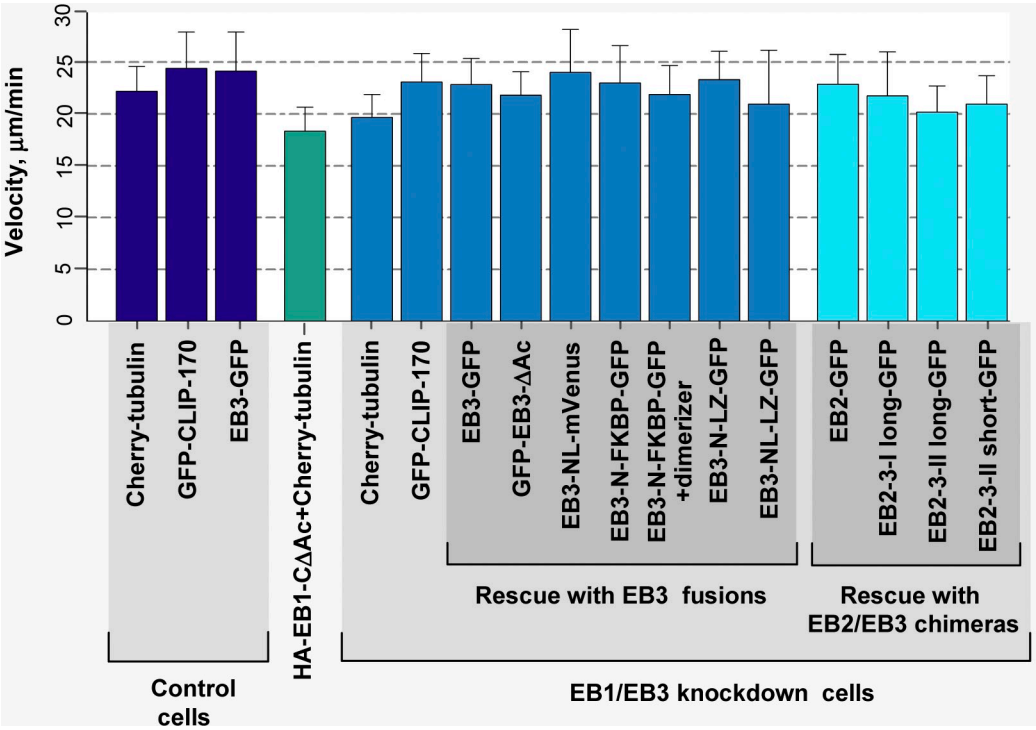

Figure S5. **MT growth rate in control cells, EB1/EB3-depleted cells, and after rescue with different EB3 and EB2 mutants.** MT growth rate was measured using kymographs with the same dataset as in Fig. 7. 180–600 growing MTs were analyzed for each condition. The variation between rates observed in rescue experiments is within the limits of variation between different control experiments. Error bars represent SD.

Table S1. **Crystallography data collection and refinement statistics**

	EB3n
Wavelength, Å	1.0009
Space group (No.)	P21 21 2 (18)
Resolution range, Å	50-1.4
Unit cell, *a*, *b*, and *c* in Å	47.2, 85.4, 32.2
No. of observed reflections	147682 (25226)*
No. of unique reflections	25525 (4469)*
R_{sym}[a], %	10.7 (63.2)*
I/σ (I)	10.9 (3.7)*
Completeness, %	96.9 (92.9)*
No. of refined atoms	
Proteins	1097
Water	151
R-factor/free *R*-factor[b]	0.20/0.23
RMSD bond lengths/bond angles[c]	0.01/1.1

[a] $R_{sym} = \sum_h\sum_i | I_i(h) - \langle I(h)\rangle | \,/\!/\, \sum_h\sum_i I_i(h)$, where $I_i(h)$ and $\langle I(h)\rangle$ are the ith and mean measurement of the intensity of reflection h.
[b] $R = \sum | F_P^{obs} - F_P^{calc} | \,/\!/\, \sum F_P^{obs}$, where F_P^{obs} and F_P^{calc} are the the observed and calculated structure factor amplitudes, respectively.
[c] RMSD, root-mean-square-deviation from the parameter set for ideal stereochemistry.
* Figures in parentheses indicate the values for the outer shell of the data.